Available online at www.sciencedirect.com
ScienceDirect
International Journal of Heat and Mass Transfer 51 (2008) 3794–3802
International Journal of HEAT and MASS TRANSFER
www.elsevier.com/locate/ijhmt

Natural convection in water-saturated metal foam

V. Kathare, J.H. Davidson *, F.A. Kulacki

Department of Mechanical Engineering, University of Minnesota, 111 Church Street, S.E., Minneapolis, MN 55455, United States

Received 27 August 2007; received in revised form 21 November 2007
Available online 7 March 2008

Abstract

Natural convection in water-saturated copper foam is measured for $2.5 \times 10^{-4} < Da < 1.2 \times 10^{-5}$, $10 < Ra_m < 210$, and $7.5 \times 10^5 < Ra_f < 2.5 \times 10^8$. Experiments are reported for foam with 92% porosity and 10 and 20 pores per inch. The primary finding is that the Nusselt numbers do not follow the published heat transfer correlations with Rayleigh number for a packed bed of spheres and are 27–42% less than that predicted by these correlations at the maximum Rayleigh numbers encountered for $Da \sim 10^{-5}$. A single heat transfer correlation of Nusselt number is obtained in terms of Rayleigh and a modified Prandtl number equal to $Pr_m Da^{-1/2} C_f^{-1}$. In comparison to natural convection in a water layer, enhancement of heat transfer is primarily via conduction. Enhancement of the advective component of heat transfer is obtained only for $Ra_f \sim 10^8$ and $1.2 \times 10^{-5} \leqslant Da \leqslant 2.4 \times 10^{-5}$.

Keywords: Natural convection; Metal foam; Porous media

1. Introduction

The use of metal foam in heat exchange applications is relatively recent, and commercially viable technology is yet under development and the subject of fundamental and applied research. Metal foam saturated with water can enhance both stagnant thermal conductivity and convective transport, but the relative importance of each has not been fully quantified and characterized for either forced or natural convection. The present paper was motivated by an interest in the application of metal foam in sensible heat water storage systems that operate on a charge–discharge cycle and rely on natural convection to deliver and remove energy via immersed heat exchanger(s). Our hypothesis is that the presence of the foam will enhance heat transfer coefficients in such systems and thus improve the rate of both energy storage and release. As a first step toward technology development, the heat transfer law for steady convection in saturated foam is needed. Based on the work of Liu et al. [1] for immersed tubes and tube bundles in a thermal store, the steady state heat transfer law is an adequate tool for system characterization owing to the low convective velocities and time scales associated with charge and discharge.

A metal foam is a porous medium with high surface area per unit volume, high bulk porosity ($\varepsilon > 0.9$), and a structure characterized by thin fibers, or ligaments, of metal joining several others in a random manner throughout the volume. Another important parameter is pore density, commonly expressed as pores per inch (PPI). Metal foams are available in a range of PPI, with 5, 10, 20 and 40 PPI ratings. Metal foam made of high conductivity metals, e.g., copper and aluminum, can be used to enhance heat transfer when the material is applied to a surface, e.g., heat sinks and tubular heat exchangers. In a convective heat transfer application, both fluid mechanical effects and the thermophysical properties play a role in the enhancement or decrease of the convective heat transfer coefficient under a given operating condition.

The stagnant thermal conductivity of saturated metal foam has been the subject of both experimental and theoretical research [2–4], but the relation of the conductivity to pore density, porosity, and thermal conductivity ratio,

* Corresponding author. Tel.: +1 612 626 9850; fax: +1 612 625 6069.
E-mail address: jhd@me.umn.edu (J.H. Davidson).

0017-9310/$ - see front matter © 2008 Elsevier Ltd. All rights reserved.
doi:10.1016/j.ijheatmasstransfer.2007.11.051

Nomenclature

A	aspect ratio, D/L
A_m	cross-sectional area of the metal foam
c_p	specific heat at constant pressure
C_f	Forcheimer coefficient
d_p	pore diameter
Da	Darcy number, K/L^2
E	enhancement factor, Eq. (4)
E_{adv}	advective enhancement factor, Eq. (5)
k_f	thermal conductivity of fluid
k_d	dispersion conductivity
k_m	stagnant thermal conductivity
K	permeability
L	layer thickness
Nu_f	average Nusselt number based on fluid property, $qL/(A_m\Delta T)k_f$
Nu_m	average Nusselt number based on k_m, $Nu_f k_f/k_m$
Pr	Prandtl number, $\mu c_p/k$
Pr_e	effective Prandtl number, $Pr_m Da^{1/2}/C_f$
Pr_m	porous medium Prandtl number, $\mu c_p/k_m$
Pr_p	modified Prandtl number, $Pr_m Da^{-1/2}/C_f$
q	heat transfer
Ra_f	Rayleigh number based on the fluid properties, $g\beta_f(T_h - T_c)L^3/(\alpha\nu)_f$
Ra_m	porous medium Rayleigh number, $Ra_f Da\lambda$
Re_K	Reynolds number based on the permeability, $\rho_f u\sqrt{K}/\mu_f$
R^2	square of the regression correlation coefficient
t	time
T	temperature
u	Darcy velocity

Greek symbols

α	thermal diffusivity
B	thermal coefficient of expansion
δ_T	thermal boundary layer thickness
ΔT	temperature difference between the hot and the cold surfaces, $T_h - T_c$
ε	porosity
ρ	density
μ_f	viscosity
μ'	effective viscosity
ν	kinematic viscosity
λ	conductivity ratio, k_f/k_m

Subscripts

c	cold, refers to the temperature of the bounding surface
e	equivalent
f	fluid
h	hot, refers to the temperature of the bounding surface
s	solid
m	foam–water medium

k_s/k_f, is a subject of continuing study. A number of studies have been conducted on enhancement of forced convection with metal foam e.g., [5–12], but only a few investigators have reported studies of natural convection in metal foams [13–16] for the geometry and thermal boundary conditions relevant to the present study.

Calmidi and Mahajan [2] developed a one-dimensional model for the stagnant thermal conductivity of aluminum foam with air and water as the interstitial fluids. They assumed the foam structure to comprise periodic hexagonal unit cells. Their model was validated experimentally, and a correlation for the conductivity was developed in terms of k_s/k_f and ε. Bhattacharya et al. [3] replaced the cubic intersection of the ligaments with a spherical intersection, which results in sixfold rotational symmetry. They estimated the geometric parameter required by the model by visual inspection. They proposed an empirical expression for k_m using their data for reticulated vitreous carbon and the data of Calmidi and Mahajan [2]. Boomsma and Poulikakos [4] modeled the structure as tetrakaidecahedrons (single complete cells consisting of six squares and six hexagons) with the ligaments represented by thin cylinders joined at cubic nodes. Their model predicts that when there is a large difference between the solid and the fluid conductivity, the stagnant conductivity is dominated by that of the solid even at high porosity. These studies indicate stagnant thermal conductivity is independent of pore density.

Phanikumar and Mahajan [13] report experiments and numerical analysis of buoyancy induced flow in a high porosity metal foam block heated from below and surrounded on all other faces by fluid. Their numerical model is based on local thermal non-equilibrium and includes form drag and viscous (Brinkman) terms in the momentum equation. They modeled aluminum–air, aluminum–water, nickel–water and reticulated vitreous carbon–air foams with PPI from 5% to 40% and porosity from 89% to 97%. The key result of their analysis is that the effects of local thermal non-equilibrium (LTNE) are significant. Comparison of the fluid Nusselt numbers (Nusselt number based on the conductivity of the fluid alone) with and without metal foam indicates that the aluminum foam–water combination produces the highest enhancement (16 times that without foam) in heat transfer coefficient, followed by the nickel foam–water combination (9.5 times) and then the aluminum foam–air combination (3.8 times). From their experiments with aluminum–air, heat transfer rate increases as the porosity and the pore density are

decreased. A decrease in porosity increases metal content and hence increases the stagnant conductivity, whereas a decrease in pore density reduces the flow resistance.

Zhao et al. [14,15] report experiments and a numerical study of Bénard equivalent convection in steel alloy foam with air as the interstitial fluid. In both the experiments and analysis, the effects of Darcy and Rayleigh numbers are sought for foam of 30–90 PPI and 5% and 10% relative density. Their analysis [15] is based on LTNE, and owing to the lack of a reliable correlation for the Forcheimer coefficient, C_f, and the small velocities inherent in natural convection, they neglect the form drag term in the momentum equation but include dispersion based on the work of Georgiadis and Catton [17]. They find that for a given foam–fluid combination and for a given fluid Rayleigh number, a critical value of Da exists which signals an increase of the effective conductivity, i.e., the initiation of convection. For larger Da, the effective thermal conductivity approaches a steady value asymptotically, which implies that the natural convection in a foam–fluid combination behaves the same as that in a fluid layer with conductivity equal to the stagnant conductivity of the medium. For $Ra_m > 100$, Nu_m increases with Ra_f for a constant value of Ra_m. The authors conclude that the effect of increasing buoyancy at higher Ra_f is greater than the effect of decreasing Da on convective transport. Their model of thermal conductivity agrees with measured data [14] to within 28%.

Krishnan et al. [16] modeled the effects of LTNE in a side heated two-dimensional foam filled cavity with $k_s/k_f = 10^3$, $10^5 \leqslant Ra_f \leqslant 10^8$, $Da = 10^{-2}$ and 10^{-3}, $Pr = 1$ and 100, and $d_p/L = 0.0135$. Although their boundary conditions are not those of the present study, their results suggest that LNTE and the resulting inter-phase heat transfer can make a significant contribution to the temperature distributions in the solid and fluid phases. Temperature gradients in the solid and fluid likewise exhibit their greatest differences within the thermal boundary layer and then converge to zero simultaneously in the central region.

In comparison, numerous experimental and theoretical studies have been reported on natural convection in a saturated porous media comprising a packed bed heated from below [18–30]. The dependence of the Nusselt number on the Rayleigh number is well understood when the fluid pressure drop can be expressed by Darcy's law (i.e., creeping flow). For very large Rayleigh number, when the form drag is significant in determining the flow resistance of the porous medium, it has been suggested that there is an explicit dependence of Nusselt number on Rayleigh number as well as the porous medium Prandtl number and the Darcy number [25,26,28], but this aspect of natural convection in a packed bed has not been fully resolved. Further when $Re_K < 1$, the Darcy flow assumption is sufficient to describe the relation between the Darcy velocity and the pressure drop, but when $Re_K > 10$, the pressure drop is dominated by form drag (the Forcheimer effect) [31].

Metal foams produce a much different convective heat transfer problem for buoyant flow owing to their ligament structure, high porosities and high k_s/k_f ratio. Based on numerical study of forced convection over a flat plate embedded in a porous medium, Vafai and Tien [32] claim that although the boundary effect (Brinkman effect) is not significant for flow considerations, it can be significant for heat transfer. In packed beds, the effects of viscous drag are nullified by the effects of higher porosity near the wall [33]. However, for metal foam with uniform porosity and higher permeabilities, boundary effects can play a significant role in determining the heat transfer. The ligament geometry for most commercially produced metal foam is triangular [3], and estimated to produce larger pressure drop than that predicted by Darcy's law even at low velocities. This characteristic should produce lower convective transport and heat transfer. However flow separation enhances fluid mixing (dispersion). The relative importance of these competing effects in natural convection needs to be examined more fully. Moreover, there is apparently no generally accepted range of Re_K to distinguish the Darcy from the Darcy–Forcheimer regimes of convection.

The objective of the present study is to develop correlations for free convection in water-saturated copper foam. Further, the degree to which metal foam can enhance the overall heat transfer coefficient over a range of geometrical and thermophysical parameters is shown. Heat transfer measurements are reported in a cavity filled with water-saturated copper foam and heated from below. Foam layers with uniform PPI, as well as layers in which the PPI were varied in well defined sub-layers are used in the present study.

2. Apparatus and procedure

The experimental apparatus comprises a well insulated acrylic cylinder of 0.127 m ID × 0.00635 m wall thickness with a heated lower boundary and a vertically adjustable cold upper boundary (Fig. 1). A rubber coated thin flexible resistance heater (0.102 m DIA × 1.4 mm) is located beneath a copper bottom plate, and a copper cooling coil is brazed to a copper top plate. A similar guard heater and a separator plate assembly at the bottom are used to drive the applied heat flux upwards through the foam. The resistance of the heaters is 218 Ω. The top plate is held at ~288 K with a cooling coiling coil brazed to the upper surface. The upper and lower plates have sufficiently high thermal conductivity and diffusivity so that temperature variations across the surface do not exceed 0.9 K for the present experiments. A bleed valve on the upper surface allows the escape of any trapped air as the cavity is filled with de-gassed water. In operation, a layer of insulation is wrapped around the outer surface of the cylinder.

Individually calibrated Type E thermocouples (Chromega$^{(T)}$-constantan) made of high grade 36 Ga wire were used for temperature measurements on the upper and lower surfaces. Each of these surfaces is a 9.53 mm thick copper plate with six thermocouple wells in each. For each plate, thermocouple junctions are located 0.53 mm beneath the

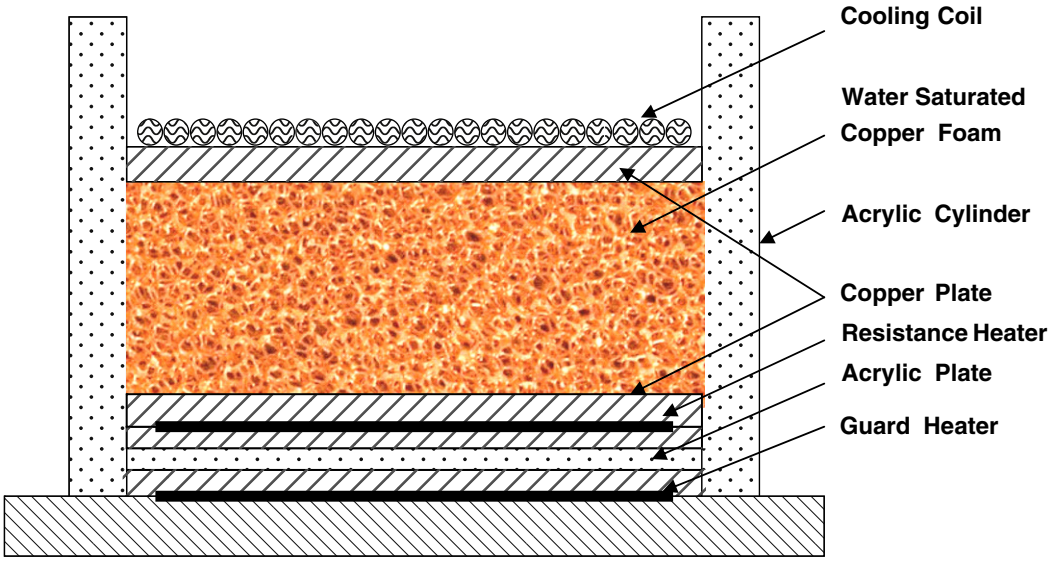

Fig. 1. Cross section of experimental apparatus.

surface in contact with the metal foam–water medium. Three thermocouples are located at a radius of 12.7 and three at 38.1 mm. Similarly positioned thermocouples are located on the bottom plate beneath the surface. Six thermocouples are located on each side of the acrylic separator plate (Fig. 1). These measurements are used to determine heat loss through the bottom of the apparatus [34]. Three thermocouples are fixed to the exterior surface of the cylinder to estimate heat loss through the sides. Heat loss was estimated by assuming 1-D radial heat conduction through the cylinder walls. Net heat flux through the metal foam–water medium was determined by subtracting heat loss through the cylinder wall and bottom plate from the power setting of the primary heater. For the range of applied power in the present experiment, heat losses were on the order of 6% or less. All thermocouples are mounted with Omega Bond®101 ($k = 1$ W/m K). An ice bath provides a single reference temperature for all thermocouple measurements. Temperatures of the bounding surfaces were recorded at steady state for $t > 2$ h, and average temperatures on the upper and lower surfaces were used to determine the Rayleigh and average Nusselt numbers. The thermocouples were calibrated along with the data acquisition hardware using a high precision RTD. This procedure reduced the measurement uncertainty of each thermocouple to ± 0.04 K. The uncertainty in the mean temperature of the isothermal boundaries includes the calibration uncertainty as well as the statistical error due to averaging temperatures along the surfaces. The total uncertainty is ± 0.9 K at the 95% confidence level.

Open cell copper foam disks made by ERG Aerospace, Inc. each 0.0127 m DIA $\times$ 0.0254 m and rated at 10 and 20 PPI and $91.6 \pm 0.2\%$ porosity were stacked within the cylinder. Thermal bonding of the foam to the top and bottom plates was assured by $\sim$0.2 mm of thermal paste ($k = 2.3$ W/m K). The thermal conductivities of the copper alloy and water at room temperature are 391 and 0.58 W/m K, respectively and thus $\lambda \sim 0.07$. The overall Darcy number was varied by stacking the multiple foam disks to change the layer thickness, L, and by ordering the foam cylinders to change the PPI distribution within the overall foam layer (Table 1). The Rayleigh number was varied by changing the heat flux from 1280 to 5213 W/m^2 and by

Table 1
Foam layers with PPI distributions and key descriptive and dimensionless parameters

Foam layer	A	ε	$d_p \times 10^3$ m	$K \times 10^7$ m$^2 \pm 0.1$	$C_f \pm 0.005$	k_m W/m K ± 0.44	$Da \times 10^5$	$Ra_f \times 10^{-6}$	Ra_m	Pr_m
10 PPI ($L = 0.0254$ m)	5	0.92	2.54	1.6	0.068	8.83	25.4	0.75–2.6	12–44	0.49–0.54
20 PPI ($L = 0.0254$ m)	5	0.92	1.25	1.1	0.083	8.85	16.5	1.9–4.6	21–51	0.40–0.44
10 PPI ($L = 0.0508$ m)	2.5	0.92	2.54	1.6	0.068	8.83	6.3	10–29	44–122	0.44–0.54
20 PPI ($L = 0.0508$ m)	2.5	0.92	1.25	1.1	0.083	8.85	4.1	17–40	43–113	0.41–0.45
10 PPI–20 PPI–10 PPI (each 0.0254 m thick; $L = 0.0762$ m)	1.67	0.92	2.54	1.4	0.074	8.83	2.4	49–100	73–196	0.40–0.49
20 PPI–10 PPI–20 PPI (each 0.0254 m thick; $L = 0.0762$ m)	1.67	0.92	1.25	1.2	0.078	8.84	2.1	54–153	75–216	0.37–0.41
10 PPI–20 PPI–20 PPI–10 PPI (each 0.0254 m thick; $L = 0.1016$ m)	1.25	0.92	2.54	1.3	0.076	8.84	1.2	110–254	94–212	0.45–0.49

changing the layer thickness, L. Aspect ratios fall in the range $1.25 \leqslant A \leqslant 4$, with $0.0254 \leqslant L \leqslant 0.1016$ m.

The stagnant thermal conductivity of the 10 and 20 PPI foams, k_m, was determined via measurement of heat transfer with a stable temperature gradient, i.e., heating from above. To determine the permeability and the form drag coefficient, pressure drop was measured across the foam in an air-flow channel with Darcy velocities from 0.04 to 1 m/s. The reported values of K and C_f were obtained from a regression analysis in the form of a quadratic expression for pressure drop per unit depth of foam. The stagnant thermal conductivity, the permeability and the Forcheimer coefficient of each layer combination are reported in Table 1 along with measurement uncertainty. Maximum measurement uncertainties in computed Darcy, Rayleigh, and Nusselt numbers are 8%, 13% and 12%, respectively. Uncertainty in both Ra_f and Nu_f are 11%.

3. Results

3.1. Heat transfer correlations

Natural convection in a water layer (without foam) was determined to validate the experimental design and to ensure wall effects are insignificant. Steady state Nusselt numbers are well correlated by

$$Nu_f = (0.10 \pm 0.02) Ra_f^{0.31 \pm 0.01}, \quad (1)$$

where $4 \times 10^5 < Ra_f < 3 \times 10^8$, and $R^2 = 0.996$. Fig. 2 shows the present data and the correlation of Garon and Goldstein [35] are in good agreement.

Fig. 3 shows the measured Nusselt and Rayleigh numbers in comparison to Elder's correlation, $Nu_m = Ra_m/40$, for a packed bed of spheres [21]. The Nusselt numbers predicted by Wang and Bejan's correlation [28] match those predicted by Elder's correlation for the present range of Ra_m and Da. The data for layers in which the 10 and 20 PPI are adjacent to the isothermal boundaries are distinguished on the plot by open and closed symbols, respectively. For $Da = 25.4 \times 10^{-5}$ and 16.5×10^{-5}, the onset of convection can be observed at $Ra_m \sim 40$; for $Ra_m \leqslant 40$, $Nu_m = 1$. For $Da < 10^4$, $Ra_m \leqslant 40$ was not obtained experimentally due to unacceptable measurement uncertainty at low heat flux. The onset of convection at $Ra_m \sim 40$ is in agreement with linear stability analysis [19], and measurements obtained in several other experimental studies. Further the present data suggest the destabilizing effect of the aspect ratio ($1.25 < A < 4$) [15] is nullified by the stabilizing effect of low thermal conductivity ratio ($\lambda \sim 0.07$), which delays the onset of convection [29]. For each PPI, Nu_m increases with decreasing Da at a given Ra_m. An explanation for this result lies in the definition of the porous medium Rayleigh number. For a fixed Ra_m, Ra_f increases as the Da is decreased. The effect of a decrease in Da is an increase in the flow resistance. But the effect of an increase in Ra_f is an increase in the buoyancy force. Thus, the present results suggest that the effects of increased buoyancy on heat transfer are stronger that the effect of the increased resistance to flow. This interpretation agrees with the numerical work of Zhao et al. [15]. Fig. 3 also shows that for each Da and PPI, the Nusselt number falls below the trend of the packed bed correlation at sufficiently large Ra_m. There is a distinct difference in the trends for the layers in which the 10 and 20 PPI foam are adjacent to the boundaries.

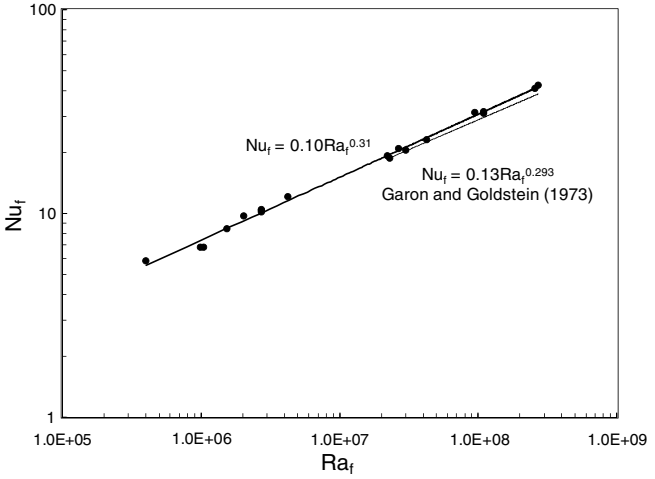

Fig. 2. Measured Nusselt number for natural convection in a water layer (Eq. (1)) compared to the correlation of Garon and Goldstein [35].

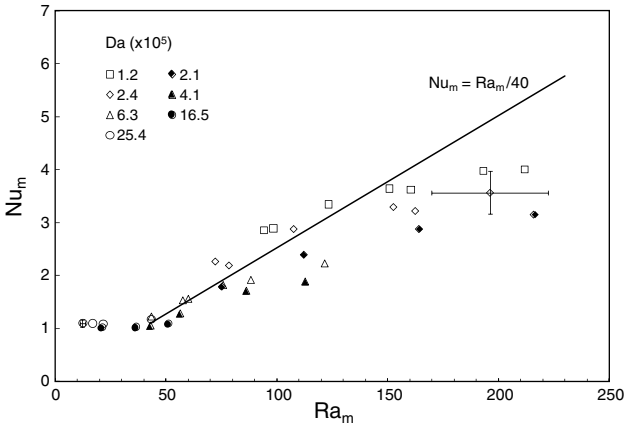

Fig. 3. Measured heat transfer data in water-saturated copper foam, plotted in terms of Nu_m versus Ra_m and correlations of Elder, $Nu = Ra_m/40$ [21] (note that the correlation of Wang and Bejan [28] coincides with Elder's for these Ra_m). In this and the following figures, open symbols correspond to the experiments performed on 10 PPI foam or on a layer with 10 PPI foam adjacent to the boundaries. Closed symbols correspond to the experiments performed on 20 PPI foam or on a layer with 20 PPI foam adjacent to the boundaries. Maximum and minimum values of uncertainty are shown.

As shown in Fig. 4, the data for both 10 and 20 PPI are well correlated in the form suggested by dimensional analysis in which a modified Prandtl number [28], $Pr_p = Pr_m Da^{-1/2}/C_f$, is introduced,

$$Nu_m = (0.007 \pm 0.005) Ra_m^{0.54 \pm 0.08} Pr_p^{0.48 \pm 0.10}, \quad (2)$$

where $44 \leqslant Ra_m \leqslant 216$, $379 \leqslant Pr_p \leqslant 1818$, and $R^2 = 0.960$. Eq. (2) successfully correlates the 10 and 20 PPI data onto

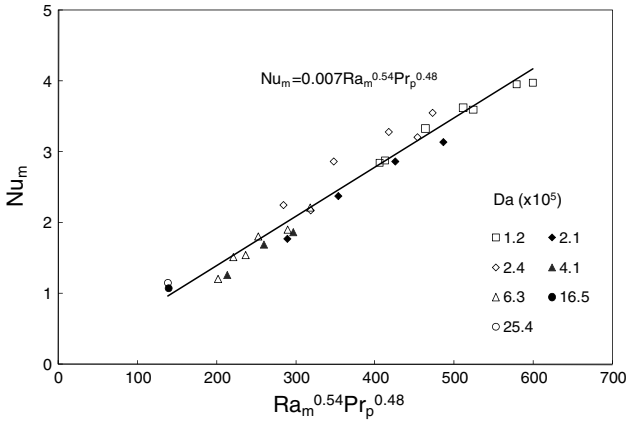

Fig. 4. Overall heat transfer correlation of the present data.

a single relation. Alternatively, the data can be correlated using the product of the fluid Rayleigh number and the conductivity ratio, and the effective Prandtl number [26],

$$Nu_m = (0.006 \pm 0.004)(Ra_f \lambda)^{0.53\pm0.09} Pr_e^{0.6\pm0.2}, \quad (3)$$

where $2.6 \times 10^6 \leqslant Ra_f \leqslant 2.54 \times 10^8$, $0.02 \leqslant Pr_e \leqslant 0.11$, $0.065 \leqslant \lambda \leqslant 0.068$ (based on temperature variations), and $R^2 = 0.960$.

3.2. Heat transfer enhancement

The practical goal of inserting metal foam into a water layer is to increase heat transfer coefficients over those obtainable with water alone. Thus, a measure of heat transfer enhancement can be seen if the present data are cast in terms of the Nusselt and Rayleigh numbers using fluid properties. Fig. 5 shows Nu_f versus Ra_f, along with Eq. (1) for a water layer. For any given Ra_f, the fluid Nusselt number obtained with foam is larger than that for the water layer with the exception of a single measurement ($Da = 4.1 \times 10^{-5}$, $Ra_f = 1.6 \times 10^7$).

For $Da = 25.4 \times 10^{-5}$ and 16.5×10^{-5}, Nu_f remains nearly constant even with an increase in Ra_f. This behavior suggests heat transfer via conduction. In these cases, $Ra_m \leqslant 40$, and heat transfer enhancement is a result of the high stagnant conductivity of the water-saturated copper foam. However, for the remainder of the present data, Nu_f increases with increasing Ra_f. Comparison of the data for $Da = 6.3 \times 10^{-5}$, which corresponds to $L = 0.0508$ m and 10 PPI foam, to the data for $Da = 4.1 \times 10^{-5}$, which corresponds to $L = 0.0508$ m and 20 PPI foam, reinforces the fact that heat transfer enhancement with 10 PPI foam is greater than that with 20 PPI foam.. The 10 PPI foam has less surface area compared to the 20 PPI foam but it has higher permeability. We attribute the increase in heat transfer to the increase in permeability. This conclusion is also supported by the fact that at a given Ra_f, both Nu_f and Nu_m obtained with 10/20/10 PPI layering ($Da = 2.4 \times 10^{-5}$) are larger than values obtained with 20/10/20 PPI layering ($Da = 2.1 \times 10^{-5}$).

To quantify the increase of heat transfer coefficient with foam, an enhancement factor at a given fluid Rayleigh number is defined as

$$E = \left.\frac{(Nu_f)_{foam}}{(Nu_f)_{no\ foam}}\right|_{Ra_f} = \left.\frac{q}{(0.10Ra_f^{0.31})k_f A_m \frac{\Delta T}{L}}\right|_{Ra_f}. \quad (4)$$

Enhancement factors are shown in Fig. 6 as a function of Ra_f. In general, $E > 1$ and increases with increasing Ra_f when $Ra_m > 40$. However, when $Ra_m \leqslant 40$ ($Da = 25.4 \times 10^{-5}$ and 16.5×10^{-5}), E decreases with increasing Ra_f. In this case, prior to the initiation of convection, the fluid Nusselt number with foam remains almost constant (Fig. 5), whereas the Nusselt number in a water layer without foam increases with increasing Ra_f. For $Da = 4.1 \times 10^{-5}$ and $Ra_f = 1.6 \times 10^7$, $E < 1$, which suggests suppression of convective heat transfer with foam. It is also seen that the values

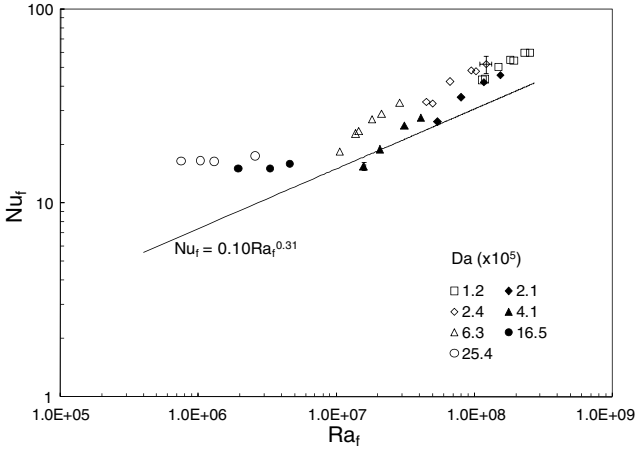

Fig. 5. Fluid Nusselt numbers with metal foam. The correlation shown is that for water without foam. Measurement uncertainties are maximum and minimum values.

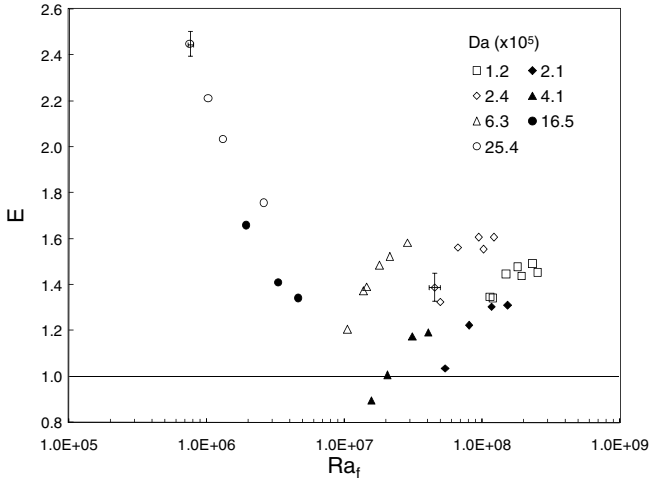

Fig. 6. Heat transfer enhancement with foam compared to heat transfer in a water layer without the foam. Measurement uncertainties are maximum and minimum values.

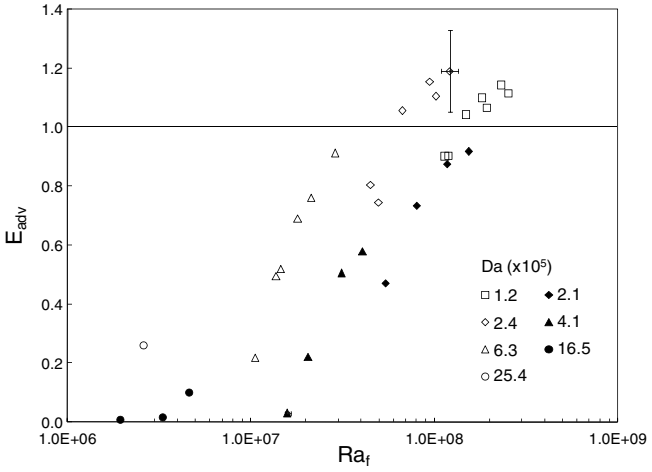

Fig. 7. Enhancement of advective heat transfer with foam compared to that in a water layer without the foam. Measurement uncertainties are maximum and minimum values.

of E for $Da = 4.1 \times 10^{-5}$ are less than the values for $Da = 6.3 \times 10^{-5}$, which supports the assertion that the 20 PPI foam suppresses convective heat transfer.

Another measure of heat transfer enhancement is the comparison of heat transfer with and without foam on the basis of the increment above conduction due to advective transport at a given Ra_f. For this purpose, the enhancement factor is,

$$E_{adv} = \left.\frac{q - k_m A_m \frac{\Delta T}{L}}{\left(0.10 Ra_f^{0.31} k_f A_m \frac{\Delta T}{L}\right) - k_f A_m \frac{\Delta T}{L}}\right|_{Ra_f} = \left.\frac{(Nu_m - 1)k_m}{(0.10 Ra_f^{0.31} - 1)k_f}\right|_{Ra_f}. \quad (5)$$

When $E_{adv} > 1$, advective heat transfer contributes to the enhancement. As shown in Fig. 7, overall, E_{adv} increases with Ra_f. However, $E_{adv} > 1$ only for $Da = 1.2 \times 10^{-5}$ (10/20/20/10 PPI, $L = 0.1016$ m) and 2.4×10^{-5} (10/20/10 PPI, $L = 0.0762$ m). Otherwise, $E_{adv} < 1$, indicating that the presence of foam suppresses advective heat transfer even though the total heat transfer is enhanced, i.e., $E > 1$ (Fig. 6). For example, for $Da = 6.3 \times 10^{-5}$ and $Ra_f = 2.9 \times 10^7$, $E_{adv} = 0.9$ even though $E = 1.6$. Thus, for this combination of parameters, heat transfer enhancement is due to the high thermal conductivity of the metal foam relative to that of water.

4. Discussion

As seen in Fig. 3, at a given Darcy number, the Nusselt number at high Rayleigh number lies below the correlations proposed by Elder [21] and Wang and Bejan [28]. Possible reasons for the measured decrease are the significance of form drag and the viscous drag due to macroscopic boundary layer formation (boundary effects) at high Rayleigh numbers [25,26,28,32], the disruption of local thermal equilibrium conditions [22,27], and thinning of the thermal boundary layer to less than the pore scale so that the transport process near the isothermal surfaces approaches that of convection in water without foam [21].

To determine which of these probable causes is most significant for the present study, estimates of relevant parameters are summarized in Table 2. These parameters are calculated using a nominal pore diameter estimated from the definition PPI of the foam and the mean temperature across the foam layer. The thermal boundary layer thickness is approximated by $\delta_T \sim L/2Nu_m$[21], and the velocity scale is estimated from

$$\frac{\mu_f u_m}{K} + \frac{\rho_f C_f u_m^2}{\sqrt{K}} \sim \rho_f g \beta \Delta T. \quad (6)$$

Using this velocity scale, the ratio of form drag to the Darcy drag is

$$\frac{\text{Form drag}}{\text{Darcy drag}} \sim \frac{\rho_f C_f u_m^2/\sqrt{K}}{\mu_f u_m/K}. \quad (7)$$

A reasonable estimate of the viscous drag due to macroscopic boundary layer formation (the Brinkman effect) can be determined as

$$\text{Viscous drag} \sim \mu_f \frac{u_m}{(Pr_m \delta_T)^2}, \quad (8)$$

where the dynamic viscosity, μ_f, replaces the effective dynamic viscosity, μ', and $Pr_m \delta_T$ estimates the hydrodynamic boundary layer thickness. The ratio of the viscous drag due to the boundary effect to the Darcy drag is

$$\frac{\text{Viscous drag}}{\text{Darcy drag}} \sim \frac{\mu_f u_m/(Pr_m \delta_T)^2}{\mu_f u_m/K}. \quad (9)$$

The dispersion conductivity, k_d, is assumed to be of the form [5]

$$k_d = 0.025 \rho_f c_p u_m \sqrt{K}. \quad (10)$$

Table 2
The values of hydrodynamic and heat transfer parameters

Foam Layer	$\delta_T 10^{-2}$ m	$u_m \times 10^{-3}$ m/s	$k_d \times 10^{-1}$ W/m K	$\frac{\text{Form drag}}{\text{Darcy drag}}$	$\frac{\text{Brinkman drag}}{\text{Darcy drag}}$
10 PPI ($L = 0.0254$ m)	1.1–1.2	3.3	1.4	0.09	0.006
20 PPI ($L = 0.0254$ m)	1.2–1.3	3.8	1.3	0.12	0.005
10 PPI ($L = 0.0508$ m)	1.1–2.1	1.7–4.5	0.7–1.9	0.04–0.13	0.001–0.006
20 PPI ($L = 0.0508$ m)	1.5–2.5	2.2–4.2	0.8–1.4	0.06–0.13	0.001–0.003
10 PPI–20 PPI–10 PPI (each 0.0254 m thick; $L = 0.0762$ m)	1.1–1.7	1.9–4.7	0.7–1.8	0.06–0.15	0.002–0.008
20 PPI–10 PPI–20 PPI (each 0.0254 m thick; $L = 0.0762$ m)	1.2–2.2	2.0–5.1	0.7–1.8	0.06–0.18	0.002–0.006
10 PPI–20 PPI–20 PPI–10 PPI (each 0.0254 m thick; $L = 0.1016$ m)	1.3–1.8	1.9–4.0	0.7–1.5	0.05–0.11	0.002–0.004

For the present measurements, $\delta_T > d_p$. Hence, heat transfer has not reached the regime where behavior similar to that in a water layer without foam is expected. For a fixed Darcy number, Darcy drag is much greater than the form drag. As a result, the decrement of the Nusselt number below the $Ra_m/40$ correlation is not attributed to the dominance of the form drag as suggested by Wang and Bejan [28] for $Ra_m > Pr_p$. For the present experiments, the Nusselt numbers fall below Elder's correlation even when $Ra_m \ll Pr_p$. Based on the estimated value of u_m, $k_d \sim 0.14$ W/m K, whereas the measured stagnant conductivity of the water-saturated foam is ~9 W/m K. Thus, the contribution of dispersion to overall heat transfer is insignificant. Further it has been conjectured that for a packed bed of spheres, dispersion becomes insignificant as $L/d \to \infty$ [17]. In the present study, $L/d_p \gg 10$, and our results lend empirical support to this idea.

It is possible that both viscous drag due to the boundary effect and/or departure from local thermal equilibrium are responsible for the departure from Elder's correlation. Because the boundary effect can be significant, especially at large Ra_m, it could make a contribution to the observed decrease of the Nusselt number below the $Ra_m/40$ correlation. The large value of k_s/k_f in the present study suggests LTNE may play a role in the observed decrease [22,27], but quantitative estimates cannot be made.

5. Conclusion

The present experimental study characterizes natural convection in bottom heated water-saturated copper foam for $2.5 \times 10^{-4} < Da < 1.2 \times 10^{-5}$, $12 < Ra_m < 216$, and $7.5 \times 10^5 < Ra_f < 2.5 \times 10^8$. Commercially available copper foam with 10 and 20 PPI forms the solid matrix. Measured values of permeability, Forcheimer coefficient and stagnant thermal conductivity of the water–foam medium are also presented. The objective of the present study is to develop correlations for free convection in water-saturated copper foam. Further, the enhancement of heat transfer due to the presence of foam over that of a water layer without foam is evaluated under the hypothesis that the metal foam can provide increased mixing, interstitial heat transfer and a benefit of high stagnant conductivity.

The Nusselt numbers do not follow the published heat transfer correlations with Rayleigh number for a packed bed of spheres. Further, Nusselt numbers are 27–42% less than that predicted by these correlations at the maximum porous medium Rayleigh number encountered for $Da \sim 10^{-5}$.

In the conductive heat transfer regime, the water-saturated foam provides from 34% to 140% enhancement of heat transfer compared to that in a layer of water for $7.5 \times 10^5 < Ra_f < 4.6 \times 10^6$. After the onset of convection and for $Da \sim 10^{-5}$, enhancement of the heat transfer coefficient is 20–60% for $10^7 < Ra_f < 2.5 \times 10^8$ and 10 PPI foam adjacent to the isothermal boundaries, and as high as 31% for $1.5 \times 10^7 < Ra_f < 1.5 \times 10^8$ and 20 PPI foam adjacent to the isothermal boundaries.

Even though water-saturated foam can provide significant enhancement in overall heat transfer compared to water without foam, the enhancement in the advective component of heat transfer is obtained only for $Ra_f \sim 10^8$ for $1.2 \times 10^{-5} \leqslant Da \leqslant 2.4 \times 10^{-5}$. Further, the present data suggest that the 20 PPI foam at the isothermal boundaries suppresses buoyant motion and thus decreases overall heat transfer coefficients over the range of Rayleigh and Darcy numbers obtainable with the present apparatus. For either 10 or 20 PPI foam, we find reasonable estimates of heat transfer via dispersion are an order of magnitude lower than that by conduction. Hence conduction and buoyant advection are identified as the dominant modes of heat transfer for the present set of experiments. The large value of k_s/k_f (~660 at room temperature) lies at the base of this result, and we expect that lower ratios would not provide such a clear case for enhancement due to the presence of the foam for practical values of either Ra_m or Ra_f.

Acknowledgements

The support of this work by the National Renewable Energy Laboratory, the University of Minnesota's Initiative for Renewable Energy and the Environment and the US Department of Energy is appreciated.

References

[1] W. Liu, J.H. Davidson, F.A. Kulacki, Thermal characterization of prototypical integral collector storage systems with immersed heat exchangers, J. Solar Energ. Eng. 127 (2005) 21–28.
[2] V.V. Calmidi, R.L. Mahajan, The effective thermal conductivity of high porosity fibrous metal foams, J. Heat Transfer 121 (1999) 466–471.
[3] A. Bhattacharya, V.V. Calmidi, R.L. Mahajan, Thermophysical properties of high porosity metal foams, Int. J. Heat Mass Transfer 45 (2002) 1017–1031.
[4] K. Boomsma, D. Poulikakos, On the effective thermal conductivity of a three-dimensionally structured fluid-saturated metal foam, Int. J. Heat Mass Transfer 44 (2001) 827–836.
[5] M.L. Hunt, C.L. Tien, Effects of thermal dispersion on forced convection in fibrous media, Int. J. Heat Mass Transfer 31 (1987) 301–308.
[6] T.J. Lu, H.A. Stone, M.F. Ashby, Heat transfer in open-cell metal foams, Acta Mater. 46 (1997) 3619–3635.
[7] V.V. Calmidi, R.L. Mahajan, Forced convection in high porosity metal foams, J. Heat Transfer 122 (2000) 557–565.
[8] A. Bhattacharya, R.L. Mahajan, Finned metal foam heat sinks for electronics cooling in forced convection, J. Electron. Pack. 124 (2000) 155–163.
[9] K. Boomsma, D. Poulikakos, F. Zwick, Metal foam as compact high performance heat exchangers, Mech. Mater. 35 (2003) 1161–1176.
[10] C.Y. Zhao, T. Kim, T.J. Lu, H.P. Hodson, Thermal transport in high porosity cellular metal foams, J. Thermophys. Heat Transfer 12 (2004) 309–317.
[11] A.J. Fuller, T. Kim, H.P. Hodson, T.J. Lu, Measurement and interpretation of the heat transfer coefficients of metal foams, Proc. Inst. Mech. Eng. Part C: J. Mech. Eng. Sci. 219 (2005) 183–191.

[12] W.H. Shih, W.C. Chiu, W.H. Hsieh, Height effect on heat-transfer characteristics of aluminum-foam heat sinks, J. Heat Transfer 128 (2006) 530–537.
[13] M.S. Phanikumar, R.L. Mahajan, Non-Darcy natural convection in high porosity metal foams, Int. J. Heat Mass Transfer 45 (2002) 3781–3793.
[14] C.Y. Zhao, T.J. Lu, H.P. Hodson, J.D. Jackson, The temperature dependence of effective thermal conductivity of open-celled steel alloy foams, Mater. Sci. Eng. A 367 (2004) 123–131.
[15] C.Y. Zhao, T.J. Lu, H.P. Hodson, Natural convection in metal foams with open cells, Int. J. Heat Mass Transfer 48 (2005) 2452–2463.
[16] S. Krishnan, J.Y. Murthy, S.V. Garimella, A two temperature model for the analysis of passive thermal control systems, J. Heat Transfer 126 (2004) 628–637.
[17] J. Georgiadis, I. Catton, Dispersion in cellular thermal convection in porous layers, Int. J. Heat Mass Transfer 31 (1987) 1081–1091.
[18] C.W. Horton, F.T. Rodgers, Convection currents in a porous media, J. Appl. Phys. 16 (1945) 367–370.
[19] E.R. Lapwood, Convection of a fluid in a porous medium, Proc. Cambridge Phil. Soc. (1948) 508–521.
[20] K.J. Schneider, Investigation of the influence of free thermal convection on heat transfer through granular material, in: Proceedings of 11th International Congress of Refrigeration, Munich Germany, 1963, pp. 247–254.
[21] J.W. Elder, Steady free convection in a porous medium heated from below, J. Fluid Mech. 27 (1967) 29–48.
[22] M. Combarnous, Description du transfert de chaleur par convection naturelle dans une couche poreuse horizontale à l'aide d'un coefficient de transfert solide–fluide, C. R. Acad. Sci. Paris A 275 (1972) 1375–1378.
[23] Y.C. Yen, Effects of density inversion on free convection heat transfer in porous layer heated from below, Int. J. Heat Mass Transfer 17 (1974) 1349–1356.
[24] R.J. Buretta, A.S. Berman, Convective heat transfer in a liquid-saturated porous layer, J. Appl. Mech. 43 (1976) 249–253.
[25] J. Georgiadis, I. Catton, Prandtl number effect on Bernard convection in porous media, J. Heat Transfer 108 (1986) 284–290.
[26] T. Jonsson, I. Catton, Prandtl number dependence of natural convection in porous media, J. Heat Transfer 109 (1987) 371–377.
[27] M.A. Combarnous, S.A. Bories, Módelization de la convection naturelle au sein d'une couche poreuse horizontale à l'aide d'un coefficient de transfert solide–fluide, Int. J. Heat Mass Transfer 17 (1974) 505–515.
[28] M. Wang, A. Bejan, Heat transfer correlation for Bernard convection in a fluid saturated porous layer, Int. Commun. Heat Mass Transfer 14 (1987) 617–626.
[29] N. Kladias, V. Prasad, Natural convection in horizontal porous layers: effects of Darcy and Prandtl numbers, J. Heat Transfer 111 (1989) 926–935.
[30] C.R.B. Lister, An explanation for the multivalued heat transport found experimentally for convection in a porous medium, J. Fluid Mech. 214 (1990) 287–320.
[31] D.A. Nield, A. Bejan, Convection in Porous Media, Springer-Verlag, New York, 1992, p. 10.
[32] K. Vafai, C.L. Tien, Boundary and inertia effects on flow and heat transfer in porous media, Int. J. Heat Mass Transfer 24 (1981) 195–203.
[33] J.T. Hong, Y. Yamada, C.L. Tien, Effects of non-Darcian and nonuniform porosity on vertical-plate natural convection in porous media, J. Heat Transfer 109 (1987) 356–362.
[34] V. Kathare, Natural convection in water-saturated metal foam, MS thesis, University of Minnesota, Minneapolis, MN, 2007.
[35] A.M. Garon, R.J. Goldstein, Velocity and heat transfer measurements in thermal convection, Phys. Fluids 16 (1973) 1818–1825.